HYPOTHETICAL LANDSLIDE ORIGIN FOR BROWN'S FLAT, SAN GABRIEL MOUNTAINS, CALIFORNIA: EVIDENCE FROM STRUCTURAL DATA

CORTEZ, Pablo A., and NOURSE, Jonathan A., Department of Geological Sciences, California State Polytechnic University, Pomona, 3801 W. Temple Avenue, Pomona, CA 91768

Abstract

Brown's Flat is a large plateau (300,000 m^2) in the San Gabriel Mountains located approximately five miles southwest of Mt. San Antonio. It is a striking feature in this mountain range due to the sharp contrast in topography between it and the surrounding ridges and valleys. This broad, flat area protrudes from the side of a valley wall, approximately 180 meters below the ridgeline. No known literature discusses this inaccessible part of the San Gabriel Mountains. The purpose of my study was to investigate the origin of this topographic anomaly using structural data derived from the underlying crystalline bedrock. The methods used for gathering data consisted primarily of making numerous visits to the field site and measuring the orientations of the foliation and fracture planes using a Brunton compass. These data were then plotted on topographic base maps and stereonets. Outcrops were difficult to access due to excessive vegetation cover, but metamorphic bedrock was well-exposed in a few locations. Two such places were the road leading to the radio towers east of the flat and a major canyon (nicknamed "Alpha Canyon") traversing the flat on its northeast flank. Wherever the rock is exposed, it consistently shows the same kind of geometry in the planar structures contained therein. The foliations generally strike northeast, with dips ranging from 13 to 70 degrees northwest (towards or beneath Brown's Flat). About 25% of these dip shallower than the topographic slope. Crosscutting fractures have random strikes, but consistently dip steeper than 65 degrees. The most logical conclusion to be derived from this information is that the shoulder of the mountain that now makes up Brown's Flat was once a part of the ridgeline above it. However, due to probable failure along daylighting surfaces, it appears as though the high angle fractures may have weakened the rock sufficiently to cause a piece of the ridgeline to break off and slide northwestward along the foliation planes. This slump then leveled off below, forming the anomalous plateau now known as Brown's Flat.

Introduction

Among the San Gabriel Mountains' most well kept secrets is a strange topographic anomaly called Brown's Flat. It is a 300,000 m^2 plateau located approximately five miles southwest of

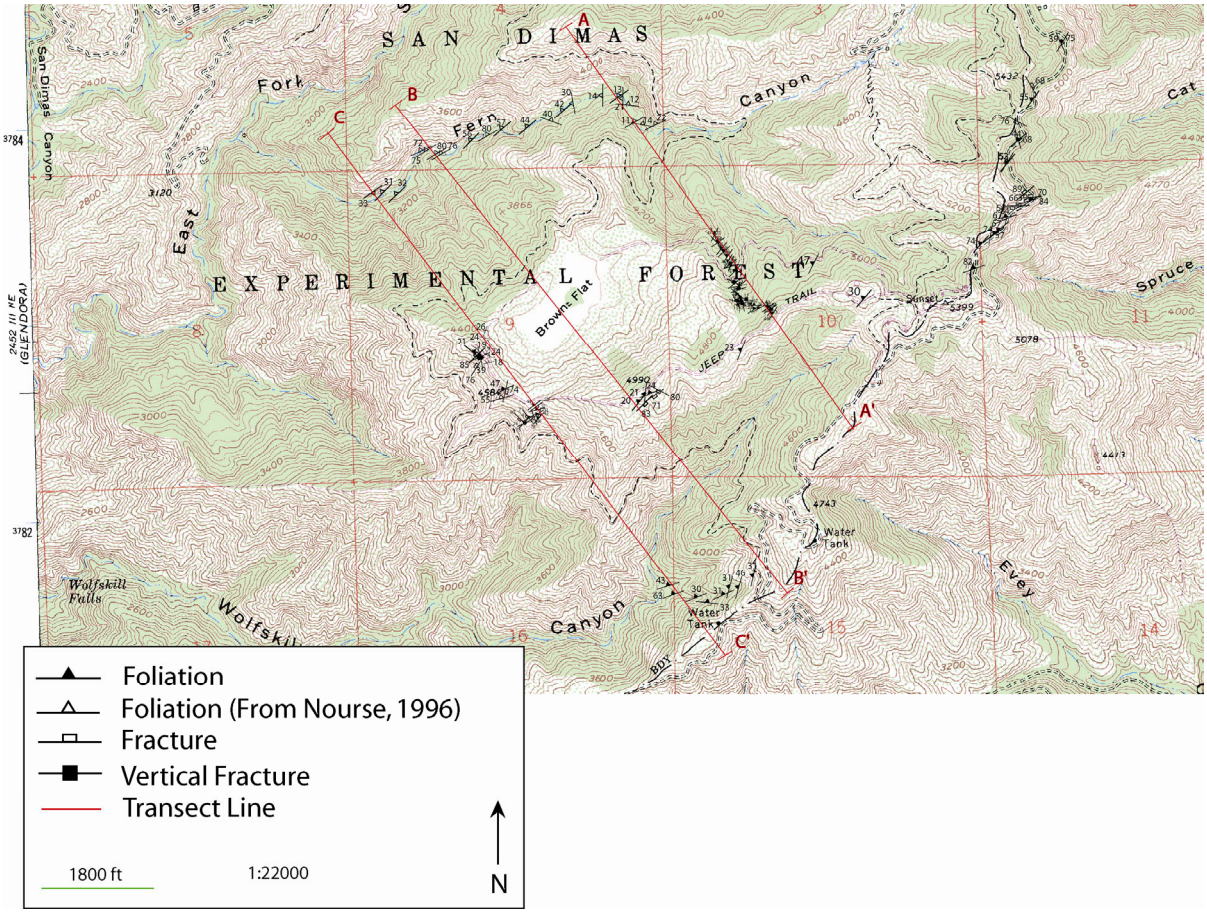

Figure 1: Generalized map of Brown's Flat and the surrounding area. Although the foliation and fracture planes may be too small to be seen here, close-up views of specific sections can be seen in Figures 3, 5, and 7. Concentrations of data points can be seen on the ridge above the flat, along Sunset Ridge Road, and in Alpha, Wolfskill, and Fern Canyons. In all areas, the foliations are generally striking to the northeast with dips to the northwest (towards Brown's Flat) that are relatively shallow. The fracture sets that are shown on the map represent fracture sets that are characterized by random strikes, but with consistently high-angle dips relative to the foliations (Nourse, et. al., 1998).

Mt. San Antonio. It is situated 180 meters below the ridgeline of the valley wall of Fern Canyon. For as long as it has been made aware of by the few who have seen it, Brown's Flat has often been carelessly given the diagnosis of being an ancient landslide deposit with little or no research to support this claim (Dibblee, 2002 and Bortugno, et. al., 1986). The purpose of this study was

to test the landslide origin hypothesis of Brown's Flat by using structural data derived from the underlying crystalline bedrock.

a. **b.**

Figure 2: a) Photograph of Brown's Flat looking to the southwest. b) Brown's Flat is viewed from the south looking north toward Mt. San Antonio. Note the heavy contrast in topography relative to its surroundings.

A discussion of the geology in the vicinity of Brown's Flat is a logical place to begin. As with the rest of the San Gabriel Mountains, the dominant rock type in the immediate vicinity of Brown's Flat is uplifted igneous and metamorphic bedrock. The igneous rocks consist mostly of course-grained Mesozoic granites, diorites, quartz diorites, and monzonites. The metamorphic rock consists of medium to course-grained Precambrian gneiss of plutonic protolith (Nourse, et. al., 1998). The dominant type of metamorphic rock is gneiss. Some of the metamorphosed plutons had schistose foliations, but a gneissic foliation was the norm for the metamorphic rock in this area. Folding in the gneiss is common in a few localities. The gneiss takes on both mafic and felsic phases and is commonly intruded by an undeformed leucocratic granite and pegmatite in several places along the fire road which branches off of Glendora Ridge Road.

To better understand the geology of the immediate area in the vicinity of Brown's Flat, a discussion of the tectonic history of the San Gabriel Mountains is warranted. The San Gabriel Mountains are part of the Transverse Ranges of Southern California, which include the San Bernardino and the Santa Rosa Mountains (Dibblee, 1982). This complex mountain range formed as a result of the compression that takes place along the bend in the San Andreas Fault. As the North American Plate moves toward the northwest at an average rate of 2.5cm/yr, the Pacific Plate moves in the same direction at an average rate of 8 cm/yr (Nourse, 2006). Because of the difference in velocity between the two plates, collision occurs at the bend in the San

Andreas Fault, causing uplift of the crust. This uplifted crust is what comprises the Transverse Ranges. Continued right-lateral faulting along the San Andreas Fault has also caused offset along this range. This is most notable in the truncation of the eastern end of the San Gabriel Mountains, which are offset to the north relative to the San Bernardino Mountains. Most of the uplift occurred since Late Miocene time (i.e., during the past 5 million years) between the San Andreas and San Gabriel Faults (Dibblee, 1982). These mountains are also home to other known landslides, such as the Hog Back Landslide in San Antonio Canyon (Herber, 1987).

Methods and Accessibility

Data gathering for this thesis was done using traditional methods of field mapping. This included making numerous visits to the field site, searching for outcropping bedrock, and measuring the strikes and dips of key planar features using a Brunton compass, namely foliation planes and fracture sets. The data was then plotted on topographic base maps in the field and later in a computer illustration program. Stereonets were used to visually discern the geometric patterns between the foliations and fractures. This information was then used to construct a total of three cross sections along three different transects through the Brown's Flat area. The necessary calculations involving safety factors were carried out as well.

A challenge to this undertaking was in the accessibility of Brown's Flat. One reason why Brown's Flat has not been studied much is because it is located in a relatively inaccessible part of the San Gabriel Mountains. It is located just off of a fire road (Sunset Ridge Road) that branches off to the south of Glendora Ridge Road. Negotiating this road required a vehicle capable of four-wheel-drive with high ground clearance. The entire area (much like the rest of the San Gabriel Mountains) was covered by thick vegetation. Sunset Ridge Road may lead to the area in the vicinity of Brown's Flat, but hiking to the flat itself required a traverse through dense brush. The dense cover made good exposures of outcrop difficult to locate, but bedrock was exposed in a few key places. These include the ridge above Brown's Flat, Sunset Ridge Road, and a major canyon which runs along its northeastern flank (which I have since come to know as "Alpha Canyon"). Figure 1 shows a map of the entire area with foliation and fracture symbols plotted. The three aforementioned areas have the highest concentrations of data. Foliations in Fern Canyon are from Nourse and others, (1996), while foliations shown in

Wolfskill Canyon are from my previous mapping expedition with Nourse during the summer of 2004.

Observations

The first visit to Brown's Flat during May of 2005 was largely a reconnaissance mission to determine the accessibility. This was also the only time that we actually hiked out to and stood on Brown's Flat itself. We did this by attempting to locate an old trail that was thought to exist which connected the road to the flat, but not much was left of this trail when we found it. It, like much of the area, was covered by thick vegetation that covered recently slumped soils. Much of the vegetation had grown back since the massive fire (Williams fire) that swept through the San Gabriels three years before. Whereas the previous year, the flat seemed barren (at least from the distance I saw it), when we arrived, the ground of the flat was covered by a dense layer of grass, weeds, and fallen pine needles. An interesting thing to note was that the flat was home to a decent number of noticeably large (~50-60 ft high) pine trees which seemed relatively unharmed by the fires. The fact that such trees were growing on Brown's Flat may suggest that a water table is present underneath the surface at a depth which is within reach of the roots of the trees. Since roots can only penetrate fractured bedrock, this served as an indication of the condition of the bedrock beneath Brown's Flat (i.e. it was most likely fractured to allow the trees access to the water table). This, however, is debatable.

The purpose of the second visit to Brown's Flat during July of 2005 was to search for outcropping bedrock along the ridgeline above the flat. Figure 3 shows a close-up of the ridgeline. The bedrock found in these outcrops (gneiss and metamorphosed plutonic rock) showed consistencies in the foliation planes. The foliations generally had a northeast strike with dips to the northwest. The shallowest of these dips was 20° and the steepest was 40°. Several fracture sets were found along these same locations. The fractures had a tendency to behave in one of two ways: they were either parallel to the foliations, or they had random strikes, but fairly high dip angles to the foliations. The latter was largely true of the larger fractures. The dips of these fractures ranged from 56° to completely vertical. All of this information was found in outcrops that were near the top on the southeast side of the ridgeline. Data gathered in this area can be seen in Figure 3.

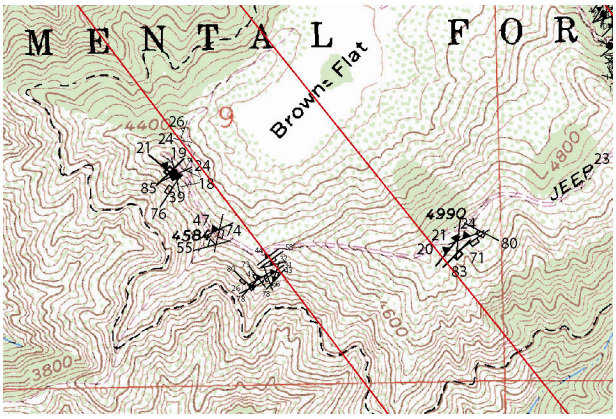

Figure 3: Close-up of the ridgeline above Brown's Flat.

a.

b.

Figure 4: a) The author measuring the foliation of the gneiss on the ridge above Brown's Flat. It is interesting to note that Brown's Flat is located on the other side of the ridge (to the right) relative to the author, meaning the gneiss is dipping towards the flat. b) Posing for aesthetic appeal.

The next visit to the field site during late summer of 2005 was focused on the bedrock which outcropped along Sunset Ridge Road. The purpose of gathering data from here was to ascertain a sense regional structure, since this was a bit farther from the flat than the ridgeline and Alpha Canyon. The foliations along the road had the same trends as those that were observed along the ridgeline. They had a general northeast strike and their dips ranged from 39-82° to the northwest (toward Brown's Flat). The fracture sets, once again, had random strikes and dips, but the dips

ranged in value from 57-89°. There were also fractures that were parallel to the foliations. Figure 5 shows a close-up view of this area on the map.

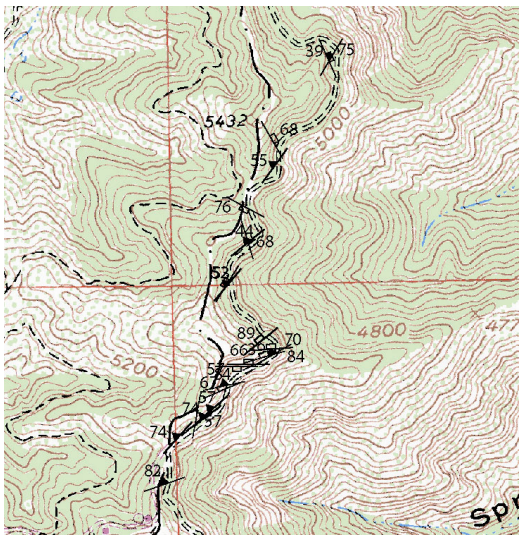

Figure 5: Close-up view of the data taken along Sunset Ridge Road.

a.

b.

Figure 6: a) Fault seen in an outcrop adjacent to Sunset Ridge Road. This is an example of a fracture that is at a high angle to the foliation in the bedrock. b) An example of folding in the gneiss.

The last visit to Brown's Flat during November of 2005 with Dr. Larry Herber had the objective to locate and traverse down Alpha Canyon. We believed that Alpha Canyon would be instrumental in determining how the bedrock is behaving beneath the surface of Brown's Flat. In Alpha Canyon, the foliations of the bedrock were found to continue the trend of northeast-striking foliations with dips to the northwest. The shallowest dip in foliation had a value of 2°,

but this was an outlier in the data. Most were in the range of 40-70° and parallel fracturing was also taking place. One of these fractures was fairly large and was daylighting out of the slope of the canyon wall. We could also see that the inside of this fracture was lined with clay. The high-angle fracture sets were present in Alpha Canyon as well. Several of theses fractures had dips that were vertical. The shallowest-dipping of these did not have dip values below 50°. As expected, they did not have any particular trend in strike and dip, other than having steep dips. Figure 7 shows the data that was found in this canyon. For photographs of this location, see Figure 8.

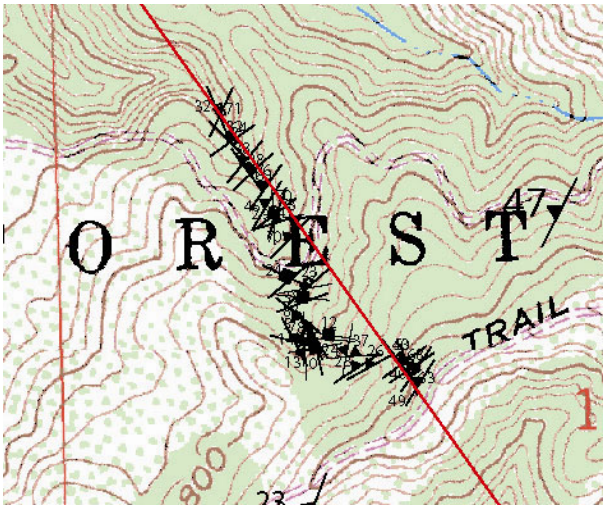

Figure 7: Close-up view of Alpha Canyon. This canyon is one of the main drainages leading into Fern Canyon and runs along the northeastern flank of Brown's Flat.

In addition to plotting the fractures and foliations on a map, the data was also plotted on stereonets to further evaluate their geometric relationships to each other. Figure 9a shows a stereonet plot of the foliation planes. As one can see, there is a large cluster of poles in the southeast quadrant of the stereonet. This means that the majority of the foliations have northeast strikes with dips to the northwest. This is of no surprise, since not only do the planes on the net demonstrate this, but the same thing was observed in the field as well. The many fractures developed parallel to this northwest-dipping foliation impart a preferred direction of weakness to the rock mass. Figure 9b shows a stereonet plot of the other fracture planes. These appear to have random orientations, but the dips have a tendency to be steep. There are no particular pole clusters, but the poles do appear to form a ring along the outer edge of the net. This is further testament to the steep nature of the dipping planes.

Figure 10 shows three cross sections of three different localities in the immediate vicinity of Brown's Flat. The transects run straight up the middle of Alpha Canyon, through Brown's Flat

itself, and along the southwest side of the ridgeline as represented by lines A-A', B-B', and C-C', respectively. Of the three cross sections shown, the most important one would be the one shown in Figure 10c. Here, we see the topographic profile of Brown's Flat and the slopes both above and below it. It is interesting to note that the slope above the flat is virtually identical to the slope below it, whereas Brown's Flat is a sharp break in that topography. The foliations show a consistent dip to the northwest. At the top of the ridge, they have a dip of approximately 20 – 24 degrees. This was the only data that was able to be ascertained along that transect, but data from Nourse (1996) is shown at the bottom of Fern Canyon and data in Wolfskill Canyon, gathered during previous research, also appears here as well. Everything between my data and that of Nourse is strictly interpolated and represents only what I believe is taking place beneath Brown's Flat. It appears that there is a small fold towards the bottom of Fern Canyon followed by an increase in the steepness of dip in the foliations. The average slope of the ground above the flat is ~25 degrees. Since the steepest foliation measured at the ridge was 24 degrees, it would appear that a daylighting condition exists on the slope above Brown's Flat. The fractures measured are shown to be at steep angles to the foliations.

Figure 10a shows a profile along the transect that runs up through Alpha Canyon. As one can see here, the same foliation trends observed on the ridge hold true for Alpha Canyon. This adds more support to the observations made in the field. There are at least two instances of folding taking place here. Data from Nourse is shown in Fern Canyon. Unlike what is shown in Figure 10c, there appears to be a decrease in the steepness of dip in the foliations; they become shallower towards the bottom. The fractures shown here are also at high angles to the foliations.

Figure 10b shows a profile along the transect that runs along the ridgeline to the southwest of Brown's Flat. The trends in the foliations and fractures do not deviate much from the other two cross sections. The only major exception to this is the syncline in Fern Canyon. This was interpolated from two foliations measured by Nourse (1996), which were dipping in opposite directions. In all three sections, there is minor folding taking place. The only exception to this is the significant syncline seen in Fern Canyon. However, this is likely to be only a local occurrence, as it does not appear in the other cross sections. The foliations continue the same northwest dips everywhere else. Data from Wolfskill Canyon indicates that this is a regional trend.

a.

b.

c.

Figure 8: Photographs from within Alpha Canyon. a) A significantly large fracture (pictured with the author and Larry Herber) was seen daylighting out of the canyon wall. Fractures like this could have made excellent slide planes if a failure occurred. b) Closeup shot of the daylighting fracture. Note that the space within the fracture appears to be filled with clay. Clay is an excellent medium for reducing the cohesion of rock that would ordinarily be considered strong (like the gneiss shown here). If this clay filling is typical of the fractures in this area, then slope failure would be a probable outcome. c) The author with Larry Herber traversing up the bedrock in Alpha Canyon. Fracturing of this bedrock parallel to the foliations can be seen here.

a.

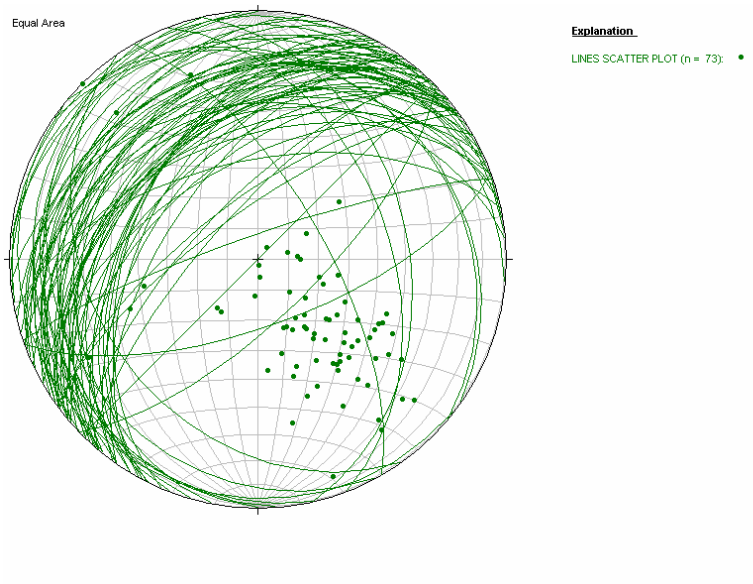

b.

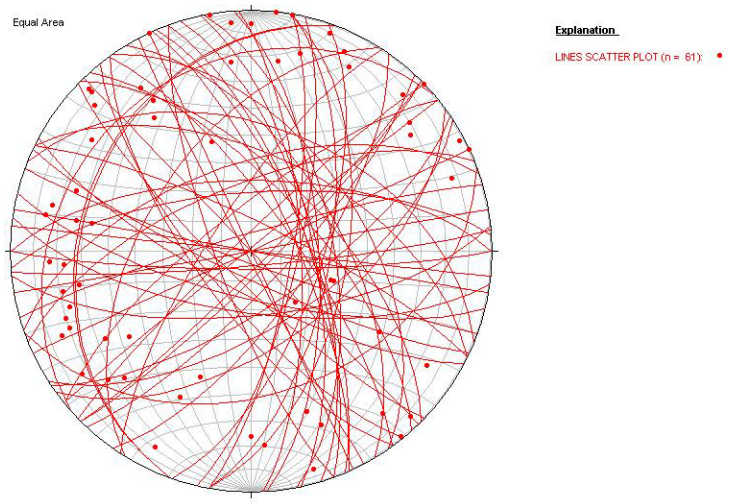

Figure 9: a) Stereonet plot showing the foliation planes. Note the dominant northeast strikes with northwest dips. This can also be seen as a representative plot for the fracture planes that run parallel to the foliations. b) Stereonet plot showing the high-angle fracture planes. The strikes are a bit more chaotic, but are consistently steep-dipping, as indicated by the pole clusters around the perimeter of the net.

Stereonet program used with kind permission from Rick Allmendinger, Cornell University.

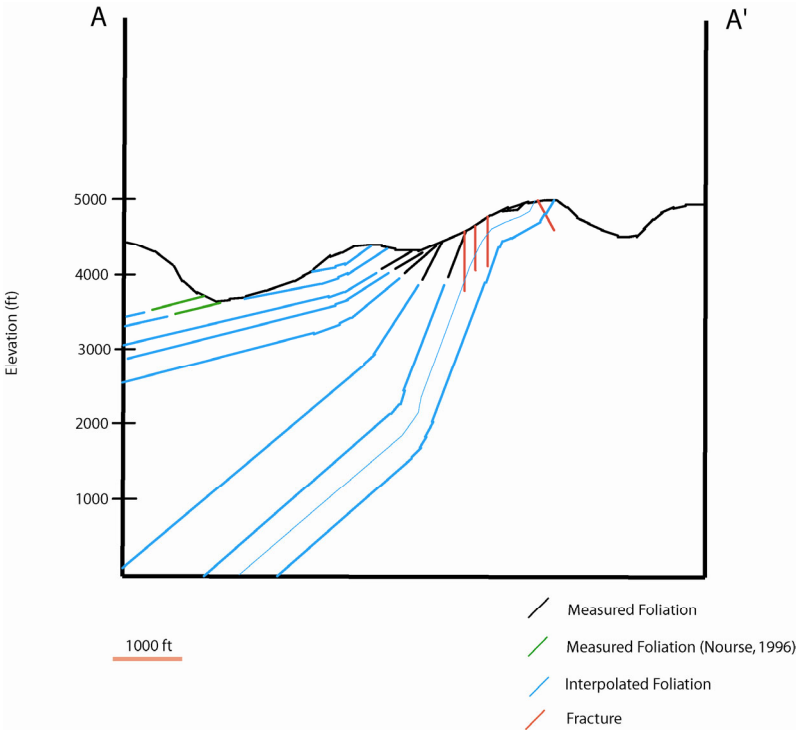

Figure 10a: Cross section along the transect that runs through Alpha Canyon. Note the northwest-dipping foliation planes. Blue lines represent the best guess as to what the foliations are doing beneath the surface. Fern Canyon is the furthermost canyon on the left. Throughout the region, there is folding is taking place to varying degrees.

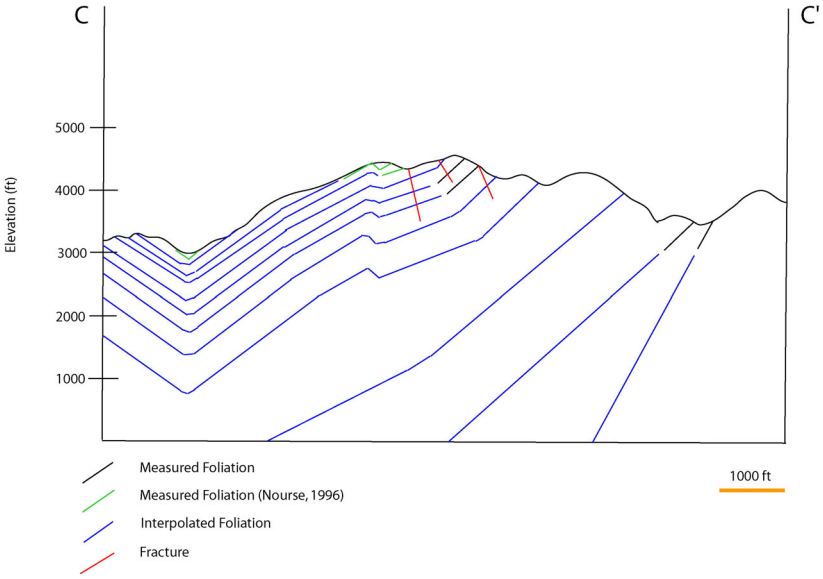

Figure 10b: Cross section of the ridge to the west of Brown's Flat. Trends in the foliations and fractures are similar to those in 3a, with the exception of the syncline in Fern Canyon. Wolfskill Canyon (furthermost canyon to the right) offers some control on the foliations as well.

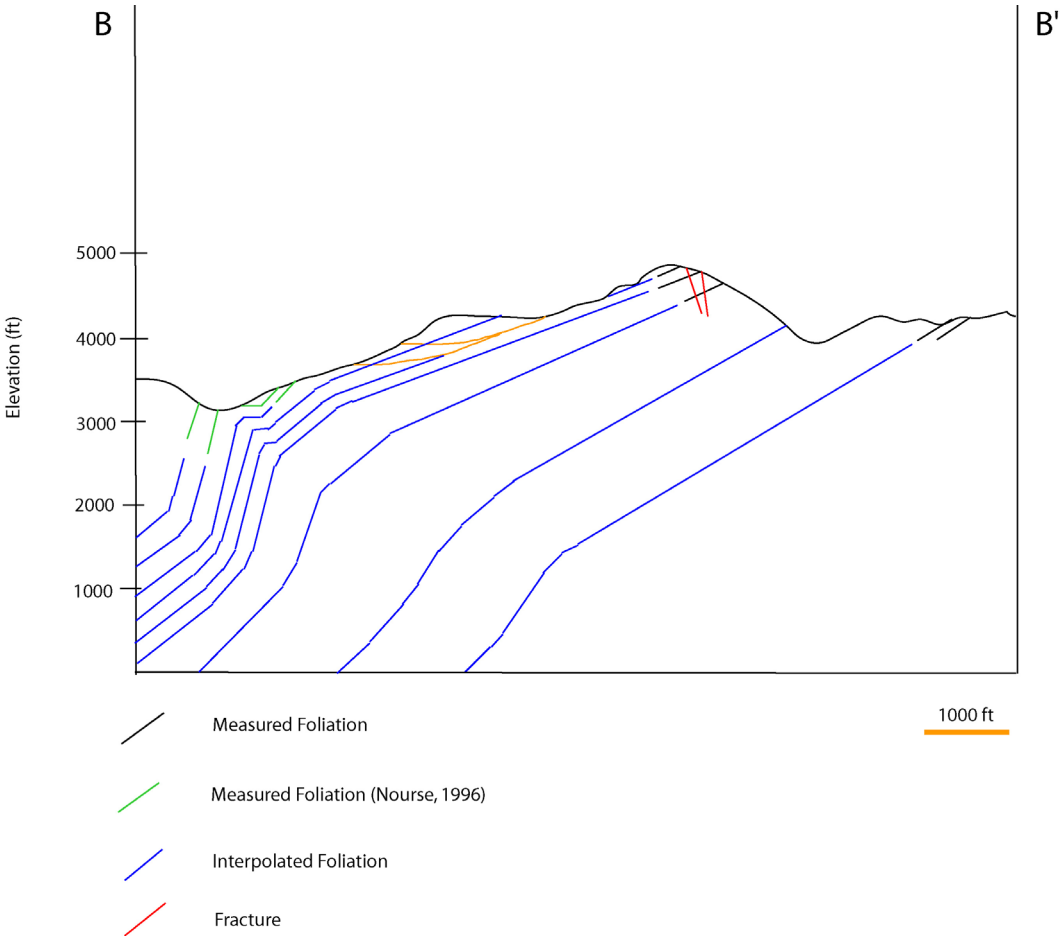

Figure 10c: Cross section through Brown's Flat (the broad, flat region located slightly above 4000 ft). The same trend of northwest-dipping planes seen in the previous two cross sections holds true here as well. The orange curves represent boundaries for two hypothetical slide masses that were assumed to be a part of the ridgeline above. These will come into prominence during the safety factor calculations, where we will assume two possible scenarios for slope failure. Also note that the slope above and below the flat are more or less identical (an average of 25°). The foliation planes on the ridge were found to have dips of no more than 24°. This means that a daylighting condition exists on the slope above the flat.

Interpretation/Discussion

Thus far, we have observed that Brown's Flat is a topographical anomaly in the San Gabriel Mountains. It is a noticeably large plateau in a landscape that is marked by a dendritic pattern of valleys, ridges, and small drainages that feed into larger drainages. The foliations of the metamorphic bedrock show consistent strikes to the northeast while dipping northwest toward the flat itself. The bedrock is fractured both parallel to the foliations and at high angles to them. This trend was seen along the fire road, along the ridgeline, and in Alpha Canyon. Visual representation of this data by maps and stereonets supports the observations made in the field. All of these clues are suggestive of a massive slope failure. Fractured bedrock has a tendency to slide along planes of bedding or, in the case of metamorphic rock, planes of foliation. If the bedrock is fractured parallel to foliation, then a slide plane is likely to develop where the fracture planes daylight. The cross sections described earlier illustrate several places where a daylighting condition exists. For example, in section B-B', Brown's Flat resides directly below a steep scarp in which daylighting foliations project through the ridge line from a point of measurement on the southeast side.

The high-angle fractures that we observed in the field could have served to further weaken the bedrock. It would appear as if the rock were broken into segments as it slid down the slope. One set of fractures cut the rock parallel to the foliations while another set cut the rock at high angles, allowing the rock to be split in a series of semi-rectangular blocks. Hypothetically, these blocks then came down one after the other en masse, and leveled off below. This is how I believe the failure occurred.

When dealing with possible slope failures, it is necessary to perform safety factor calculations. A safety factor is defined as a numerical representation of the likelihood that a failure will occur. It is generally accepted that a failure is likely for safety factors less than or equal to 1.00. Two main stresses are important when calculating a safety factor. They are the driving stress, D, and the resisting stress, R. In its simplest form, the equation for safety factor, SF, can be written as follows

1) $SF = R/D$

However, R and D can be further defined by the following equations:

2) $R = \tan\Phi[W\cos\theta/A - 1/2\gamma_{H2O}h_{max}] + C$
3) $D = W\sin\theta/A$

where Φ is the friction angle of the medium in question, W is the total weight of the slide mass, θ is the slope angle, A is the area of the slide plane, γ_{H2O} is the unit weight of water, h_{max} is the maximum vertical height in the slide mass, and C is the cohesion of the medium.

Since SF = R/D, Equations 2 and 3 can be combined to form Equation 4:

4) $$SF = \frac{\tan\Phi[W\cos\theta/A - 1/2\gamma_{H2O}h_{max}] + C}{W\sin\theta/A}$$

It is important to note that Equation 4 only holds true if water saturation is assumed to have played a part in the failure. The reason for this is because landslides occur most frequently in times of saturation, earthquakes, or both. If water were being ignored, Equation 4 would have to be modified slightly to accommodate for the absence of water, but for our purposes, this will not be done.

For this study, a total of two hypothetical scenarios were assumed. The first deals with a smaller volume of rock mass, represented on Figure 10c by the smaller area outlined in orange. This is the case which will be known as Case I. Case I assumes that the amount of slide mass which came down is as thick as this area. The volume of this mass is then obtained by multiplying the area of this section by the depth into the page (which corresponds to the width of Brown's Flat). The area of this section was approximated by dividing it into two triangles and a trapezoid. The area of each respective polygon was obtained by measuring the distances of each pertinent dimension and inserting these values into the proper area formula for each of them. Those measurements were measured in inches but multiplied by the map scale to obtain the actual real-world distances. The data derived from such calculations are as follows:

$A_1 = (273ft)(437ft)1/2 = 5.97 \times 10^4 ft^2$
$A_2 = ½(273ft + 219ft)547ft = 1.35 \times 10^5 ft^2$
$A_3 = (219ft)(656ft)1/2 = 7.19 \times 10^4 ft^2$

Those three areas, when added together, yielded the total area for the section. This area was then multiplied by the dimension into the section to obtain the volume of the hypothetical slide mass.

$A_{total} = 2.67 \times 10^5 ft^2$

$V_{total} = (2.67 \times 10^5 ft^2)(3300ft) = 8.80 \times 10^8 ft^3$

Once the total volume is obtained, a 10% porosity in the rock was assumed. This meant that the volume of pores in the rock was $8.80 \times 10^7 ft^3$ and the volume of actual rock was $7.92 \times 10^8 ft^3$. The area of the slide plane was found by measuring the length of the bottom curve and multiplying that by the dimension into the page. This led to an area of

$A_{slide\ plane} = (1750ft)(3300ft) = 5.77 \times 10^6 ft^2$

The last value to be measured was h_{max}, which was 328ft. The next step was to calculate the weight of the rock mass, W. This, of course, is assuming a case of complete water saturation, meaning water is adding significantly to this weight. When this is the case, W can be found using the following equation:

5) $W = \gamma_{rock} V_{rock} + \gamma_{H2O} V_{pores}$

Using data from Hoek and Bray (1981), γ_{rock} was set equal to 160 lbs/ft^3 while γ_{H2O} is held constant at 62.4 lbs/ft^3. The volumes for the rock and pores are the above calculated values. When all these values are plugged into Equation 5, a weight of 1.32×10^{11} lbs is the result. In this hypothetical scenario, we are assuming that the fractures are lined with clay, therefore, the cohesion, C, is set at 1000 lbs/ft^2 (Hoek and Bray, 1981). Hoek and Bray also have the friction angle of clay ranging from 7 – 27°. For this scenario, we will assume the maximum of 27°. The slope angle was actually measured as being 25°. When all of these values are inserted into Equations 2 and 3, the result is the following:

$R = \tan 27[(1.32 \times 10^{11} lbs/ft^3 \bullet \cos 25/5.77 \times 10^6 ft^2) - \frac{1}{2}(62.4 lbs/ft^3)(328ft)] + 1000 lbs/ft^2$
$= 6.35 \times 10^3 lbs/ft^2$

$D = (1.32 \times 10^{11} lbs/ft^3 \bullet \sin 25)/5.77 \times 10^6 ft^2$
$= 9.67 \times 10^3 lbs/ft^2$

These values can then be inserted into Equation 1 to obtain the safety factor.

$SF = R/D = (6.35 \times 10^3 lbs/ft^2)/(9.67 \times 10^3 lbs/ft^2) = 0.657$

As one can see, under the conditions of Case I, the safety factor is less than 1.00, therefore, a slope failure would have been likely. However, Case I represents just one possible scenario

Case I – Different Combinations

$V_{total} = 8.80 \times 10^8 ft^3$

$A_{slide\ plane} = 5.77 \times 10^6 ft^2$

$h_{max} = 328ft$

$\theta = 25°$

C (lbs/ft^2)	Φ (°)	γ_{rock} (lbs/ft^3)	Porosity (%)	Safety Factor
200	7	180	10	0.166
200	7	180	5	0.169
1000	27	160	10	0.657
1000	27	160	5	0.669
3000	27	160	10	0.864
3000	27	160	5	0.872
5000	27	160	10	1.07
5000	27	160	5	1.07
5000	7	180	10	0.609

Table 1a: Table showing different safety factors as a result of different variables. In all cases, slope failure would have been likely, as all safety factors are less than or approximately equal to 1.00.

Case I – Cohesions Resulting From Safety Factors of 1.00

Safety Factor	Φ (°)	γ_{rock} (lbs/ft^3)	Porosity (%)	C (lbs/ft^2)
1.00	7	180	10	9,242
1.00	7	180	5	9,512
1.00	27	160	10	4,318
1.00	27	160	5	4,284

Table 1b: Table showing cohesions that result when a safety factor of 1.00 is assumed for all cases. Under the conditions given, the cohesion of the medium in the rock fractures (in this case, clay) must have cohesions equal to or greater than those shown in the table in order to prevent failure.

Case II – Different Combinations

$V_{total} = 1.53 \times 10^9 ft^3$

$A_{slide\ plane} = 7.04 \times 10^6 ft^2$

$h_{max} = 437 ft$

$\theta = 25°$

C (lbs/ft^2)	Φ (°)	γ_{rock} (lbs/ft^3)	Porosity (%)	Safety Factor
200	7	180	10	0.168
200	7	180	5	0.171
1000	27	160	10	0.662
1000	27	160	5	0.675
3000	27	160	10	0.807
3000	27	160	5	0.815
5000	27	160	10	0.951
5000	27	160	5	0.956

Table 2a: Table showing different safety factors as a result of different variables. In all cases, slope failure would have been likely, as all safety factors are less than 1.00.

Case II – Cohesions Resulting From Safety Factors of 1.00

Safety Factor	Φ (°)	γ_{rock} (lbs/ft^3)	Porosity (%)	C (lbs/ft^2)
1.00	7	180	10	13,083
1.00	7	180	5	13,437
1.00	27	160	10	5,667
1.00	27	160	5	5,628

Table 2b: Table showing cohesions that result when a safety factor of 1.00 is assumed for all cases. Under these conditions, the cohesion values for the medium in the rock fractures (in this case, clay) must have cohesions that are equal to or greater than those listed in the table in order to prevent failure.

under which the slope could have failed. There are a myriad possibilities consisting of different combinations of values for the different variables in the safety factor equation. Table 1a shows several such possible combinations. It is interesting to note that even under these different conditions, the safety factor is always less than or approximately equal to 1.00. Table 1b shows a different perspective; i.e., what cohesion values are necessary to obtain a safety factor of 1.00.

The other hypothetical scenario is Case II, which deals with a larger cross sectional area and a larger slide mass volume. In Figure 10c, it would be the area bounded by the larger orange curve. Using the same methods as for Case I, the area for the section was found to be 4.65 x $10^5 ft^2$. This was then multiplied by the same distance into the page (3300ft) to get a volume of 1.53 x $10^9 ft^3$. The area of the slide plane came out to be 7.04 x $10^6 ft^2$ and the maximum height, h_{max}, was increased to 437ft. These were the only essential changes, but all the calculations were carried out the same nonetheless. Once again, we are assuming a 10% porosity. This leaves us with a porous volume of 1.53 x $10^8 ft^3$ and a rock volume of 1.38 x $10^9 ft^3$. Equation 5 is then used with these numbers in calculating the saturated weight of the rock mass.

$$W = (160lbs/ft^3)(1.38 \times 10^9 ft^3) + (62.4lbs/ft^3)(1.53 \times 10^8 ft^3) = 2.30 \times 10^{11} lbs$$

With all the above information, a safety factor can then be calculated.

$$R = \tan 27[(2.30 \times 10^{11} lbs \bullet \cos 25/7.04 \times 10^6 ft^2) - \tfrac{1}{2}(62.4lbs/ft^3)(437ft)] + 1000lbs/ft^2$$
$$= 9.14 \times 10^3 lbs/ft^2$$

$$D = (2.30 \times 10^{11} lbs)\sin 25/7.04 \times 10^6 ft^2$$
$$= 1.38 \times 10^4 lbs/ft^2$$

$$SF = R/D = 0.662$$

As with Case I, Case II also suggests a high probability of slope failure. However, as with Case I, there are many different possible combinations of variables in the safety factor equation. It is impossible to list them all, but Table 2a offers a few representative examples. Table 2b is similar to Table 1b, but using the numbers in Case II instead.

Conclusions

The hypothesis that Brown's Flat was formed by a slope failure is evidenced by many things. The first and probably the most notable piece of evidence is the fact that the foliation planes (and

their parallel fractures) dip in the direction of the flat and in general dip shallowly to moderately northwest throughout the study area. The slide mass was most likely further weakened by the high angle fractures found throughout the region. It is also interesting to note that a daylighting condition exists on the slope above the flat, as well as in Alpha Canyon. These are all conditions that are favorable for landslides to occur and this is further supported by the numbers yielded by the safety factor calculations. To further substantiate this, many different values were used in the safety factor equations and the results were unanimous. Assuming low cohesion values and friction angles typical of clays (which were assumed to mark the slide surface), all safety factors ended up being equal to or less than 1.00. The cohesions that were necessary to obtain safety factors greater than 1.0 were considerably high for clays, but within the range of possibility for stronger metamorphic rock. In light of all this, it appears likely that Brown's Flat is a landslide deposit. In order for the safety factor calculations to hold true, many things need to be assumed, but evidence from the field relationships also lends weight to the landslide hypothesis. For all these reasons, it is this author's opinion that Brown's Flat had a landslide origin.

Acknowledgements

For my professor, Dr. Jonathan A. Nourse, whose guidance made this thesis possible; Dr. Larry Herber, for his company and insight on the San Gabriel Mountains; my parents for their support and understanding; and for Emily Thompson, who inspired me to work hard to be as accomplished a scientist as she is.

References Cited

Bortugno, E.J., and Spittler, T.E., 1986, Geologic map of the San Bernardino quadrangle, California, 1:250,000: California Division of Mines and Geology Regional Geologic Map Series, Map No. 3A.

Dibblee, Thomas W., 2002, Geologic map of the Mt. Baldy quadrangle, California: Thomas W. Dibblee Foundation, Santa Barbara, California.

Dibblee, Thomas W., 1982, Geology of the San Gabriel Mountains, in Fife, D.L. and Minch, J.A., eds., Geology and Mineral Wealth of the California Transverse Ranges, Mason Hill Volume: Santa Ana, California, S. Coast Geol. Soc. Annual Meeting Symposium and Guidebook 10, p. 131-147.

Herber, Lawrence J., 1987, Hog Back: A grossly stable prehistoric rock block slide, San Antonio Canyon, Southern California: Geological Society of America Centennial Field Guide, p. 201-202.

Hoek, E., and Bray, J.W., 1981, Rock Slope Engineering, 3rd Ed., Spon Press, p. 23.

Nourse, Jonathan A., 2006, GSC 321 – Engineering Geology Lecture Notes, Spring Quarter: California State Polytechnic University, Pomona.

Nourse, Jonathan A., Morton, D.M., and Matti, J.C., 1998, Geologic map of the Mt. Baldy Quadrangle, San Gabriel Mountains, California; United States Geological Survey Open File Report 98-BDY.

Nourse, Jonathan A., 1996, Field mapping conducted in Fern Canyon, San Gabriel Mountains, California (Unpublished).